

# Image Cover Sheet

**CLASSIFICATION**

UNCLASSIFIED

**SYSTEM NUMBER**

150239

**TITLE**

WIDEBAND I/Q DEMODULATORS: MEASUREMENT TECHNIQUE AND MATCHING CHARACTERISTICS

**System Number:****Patron Number:****Requester:****Notes:****DSIS Use only:****Deliver to:** FF





National    Défense  
Defence    nationale



# **WIDEBAND I/Q DEMODULATORS: MEASUREMENT TECHNIQUE AND MATCHING CHARACTERISTICS**

by

**Jim P.Y. Lee**

**DEFENCE RESEARCH ESTABLISHMENT OTTAWA**  
REPORT NO. 1242

**Canada**

November 1994  
Ottawa





National    Défense  
Defence    nationale

# **WIDEBAND I/Q DEMODULATORS: MEASUREMENT TECHNIQUE AND MATCHING CHARACTERISTICS**

by

**Jim P.Y. Lee**  
*ESM Section*  
*Electronic Warfare Division*

**DEFENCE RESEARCH ESTABLISHMENT OTTAWA**  
REPORT NO. 1242

PCN  
011LB

November 1994  
Ottawa



## ABSTRACT

A simple I/Q demodulator which can be used to measure the amplitude, phase and instantaneous frequency of radar signals over a large bandwidth is investigated for electronic warfare applications. Imbalance errors and DC offsets are minimized by the techniques of component matching and calibration. A DFT technique is used to characterize the imbalances and DC offsets and improved matching characteristics on practical wideband demodulators are also given.

## RÉSUMÉ

Un démodulateur en quadrature de phase simple pouvant être utilisé pour mesurer l'amplitude, la phase et la fréquence instantanée de signaux radar sur une bande large est examiné pour des applications de guerre électronique. Les erreurs dues au déséquilibre et les décalages DC sont minimisés par les techniques d'égalisation des composantes et de calibrage. Une transformée de Fourier discrète est utilisée pour caractériser les déséquilibres et les décalages DC et des caractéristiques d'égalisation améliorées sont aussi données pour des démodulateurs pratiques à large bande.



## EXECUTIVE SUMMARY

Due to the increasing density and complexity of radar signal waveforms, it is becoming very difficult in electronic warfare (EW) applications to sort out and identify each radar emitter uniquely using conventional signal parameters such as pulse width, radio frequency (RF), amplitude and pulse repetition frequency. As a result, there is a requirement for EW receivers to measure precisely the modulation characteristics of radar signals in terms of amplitude, phase and/or frequency parameters. These additional parameters can then be used to identify unambiguously each type of radar emitter. With the advent of fast analog-to-digital (A/D) converters and high-speed digital signal processing technologies, it is becoming feasible to develop digital microwave processors which can meet this requirement.

One of these processors is the conventional in-phase/quadrature (I/Q) demodulator which provides three attractive features for EW applications, namely (i) wide instantaneous bandwidth (ii) simple algorithms for the extraction of modulation characteristics and (iii) a large dynamic range. However, commercially available conventional I/Q demodulators, are known to exhibit relatively large amplitude and phase imbalances and DC offsets which can introduce large systematic errors to the measurement. Other digital approaches of directly eliminating the imbalances and DC offsets have also been proposed. However, with the present state of development in both A/D converter and digital processor technologies, this simple I/Q demodulator is still very attractive for EW applications provided the imbalances and DC offsets can be kept small.

In this report, we have shown that the imbalances and DC offsets of wideband I/Q demodulators using "off-the-shelf" components can be greatly reduced and have excellent matching characteristics. This is achieved by using the techniques of component matching and through the procedure of calibration. A DFT technique is developed to calibrate and characterize accurately wideband I/Q demodulators by using a test signal. A number of wideband I/Q demodulators are evaluated over input signal power level, time and temperature and their characteristics are also reported.



TABLE OF CONTENTSPAGE

ABSTRACT/RÉSUMÉ	iii
EXECUTIVE SUMMARY	v
TABLE OF CONTENTS	vii
LIST OF TABLES	ix
LIST OF FIGURES	xi
1.0 INTRODUCTION	1
2.0 I/Q DEMODULATORS	4
3.0 CHARACTERIZATION MEASUREMENT TECHNIQUE	5
4.0 MATCHING CHARACTERISTICS OF WIDEBAND I/Q DEMODULATORS	9
4.1 Imbalances and DC Offsets Over a Range of Input Signal Power Level	9
4.1.1 100-MHz Demodulators	11
4.1.2 200-MHz Demodulators	19
4.2 Imbalances and DC Offsets Over Time and Temperature	21
5.0 COMPENSATION THROUGH CALIBRATION	22
6.0 SUMMARY AND CONCLUSIONS	23
7.0 REFERENCES	25
8.0 ACKNOWLEDGEMENTS	26



LIST OF TABLES

	<u>PAGE</u>
Table I: Imbalances and DC Offsets of Quadrature Mixer B with 10-bit Oscilloscope over a 24-dB Dynamic Range and 100 MHz-Bandwidth (10 mV/D)	16
Table II: Imbalances and DC Offsets of Quadrature Mixer B with 10-bit Oscilloscope over a 24-dB Dynamic Range and 100 MHz-Bandwidth (5 mV/D)	17
Table III: Imbalances and DC Offsets of Quadrature Mixer A with 10-bit Oscilloscope over a 24-dB Dynamic Range and 100 MHz-Bandwidth (10 mV/D)	18
Table IV: Imbalances and DC Offsets of Quadrature Mixer A with 10-bit Oscilloscope over a 24-dB Dynamic Range and 100 MHz-Bandwidth (5 mV/D)	18
Table V: Imbalances and DC Offsets of Quadrature Mixer A with 10-bit Oscilloscope over a 24-dB Dynamic Range and 235 MHz-Bandwidth (10 mV/D)	19
Table VI: Imbalances and DC Offsets of Quadrature Mixer B with 8-bit Oscilloscope over a 24-dB Dynamic Range and 200 MHz-Bandwidth (10 mV/D)	20
Table VII: Imbalances and DC Offsets of Anaren 210 Quadrature Mixer with 8-bit Oscilloscope over a 24-dB Dynamic Range and 200 MHz-Bandwidth (10 mV/D)	20
Table VIII: Imbalances and DC Offsets of Quadrature Mixer A with 10-bit Oscilloscope as a Function of Time over a Period of 30 Minutes	21
Table IX: Imbalances and DC Offsets of Quadrature Mixer A with 10-bit Oscilloscope as a Function of Time over a Period of 5 Hours	22



LIST OF FIGURES

		<u>PAGE</u>
Figure 1	Block Diagram of I/Q Demodulator	2
Figure 2	Computed Phase Deviation and Amplitude Ratio due to Leakage	8
Figure 3	Quadrature Mixers A and B	10
Figure 4(a)	Amplitude Ratio Versus Baseband Frequency of Quadrature Mixer B with 10-bit Oscilloscope over a 24-dB Dynamic Range and 100 MHz-Bandwidth (10 mV/D)	12
Figure 4(b)	Absolute Phase Difference Versus Baseband Frequency of Quadrature Mixer B with 10-bit Oscilloscope over a 24-dB Dynamic Range and 100 MHz-Bandwidth (10 mV/D)	13
Figure 4(c)	DC Offset Versus Baseband Frequency (In-phase Channel) of Quadrature Mixer B with 10-bit Oscilloscope over a 24-dB Dynamic Range and 100 MHz-Bandwidth (10 mV/D)	14
Figure 4(d)	DC Offset Versus Baseband Frequency (Quadrature Channel) of Quadrature Mixer B with 10-bit Oscilloscope over a 24-dB Dynamic Range and 100 MHz-Bandwidth (10 mV/D)	15
Figure 5	Functional Block Diagram of Compensation and Computation	24



## 1.0 INTRODUCTION

Due to the increasing density and complexity of radar signal waveforms, it is becoming very difficult in electronic warfare (EW) applications to sort out and identify each radar emitter uniquely using conventional signal parameters such as pulse width, radio frequency (RF), amplitude and pulse repetition frequency. As a result, there is a requirement for EW receivers to measure precisely the modulation characteristics of radar signals in terms of amplitude, phase and/or frequency parameters. These additional parameters can then be used to identify unambiguously each type of radar emitter. With the advent of fast analog-to-digital (A/D) converters and high-speed digital signal processing technologies, it is becoming feasible to develop digital microwave processors which can meet this requirement [1].

One of these processors is a conventional in-phase/quadrature (I/Q) demodulator shown in Fig. 1. A bandpass input signal is first down-converted to its in-phase and quadrature baseband signals and then digitized. In this figure, a dual channel digital oscilloscope is shown. The digitized data are processed to extract the modulation characteristics of the input signal. In this report, an I/Q demodulator is composed of the quadrature mixer, local oscillator (LO), low-pass filters (LPFs), signal conditioning circuitry which is used to perform functions such as gain and offset adjustments, and A/D converters. This simple demodulator can be used to measure accurately the amplitude, phase and instantaneous frequency of radar signals. It has been widely used for radar applications [2] such as digital moving target indicators and antenna array processing, where the required instantaneous bandwidth is typically a few MHz. Since the splitting of the signal into its in-phase and quadrature components is implemented using analog components, there are amplitude and phase imbalances between the two channels and DC offsets in each channel. These imbalances and DC offsets, in turn, can introduce systematic errors to the measurement [3-4]. Since the imbalances and DC offsets are relatively constant in a narrow frequency band of operation, they can thus be reduced by calibration [5-6].

With the advent of digital signal processing technologies, other approaches of directly eliminating the imbalances and DC offsets have been proposed recently [7-10]. In these approaches, the bandpass signal is either directly sampled or is first down converted to a lower intermediate frequency (IF) before it is sampled. The splitting of the input signal into its in-phase and quadrature components is carried out in the digital domain by passing the digital signal through either the digital Hilbert transform approach or a combination of mixing and filtering approach. However, the computational load of the digital processor is increased due to the additional requirements of the digital filtering operations and some distortion is introduced due to finite word length effects and the finite order of the digital filters. Moreover, for the same bandwidth coverage, the number of effective bits from an A/D converter is reduced when the digital approach is used due to the fact that the signal is required to be sampled at a higher sampling rate than for the baseband signal. As a result, the higher the rate the A/D converter is required to operate, the lower usually the effective number of bits. In addition, the effective number of bits is also reduced when the input signal frequency is increased. This is exemplified by the HP 8-bit digital oscilloscopes [11] where the effective number of bits is reduced from 7.5 at an input signal frequency of 50 KHz to 5.2 at 500 MHz.

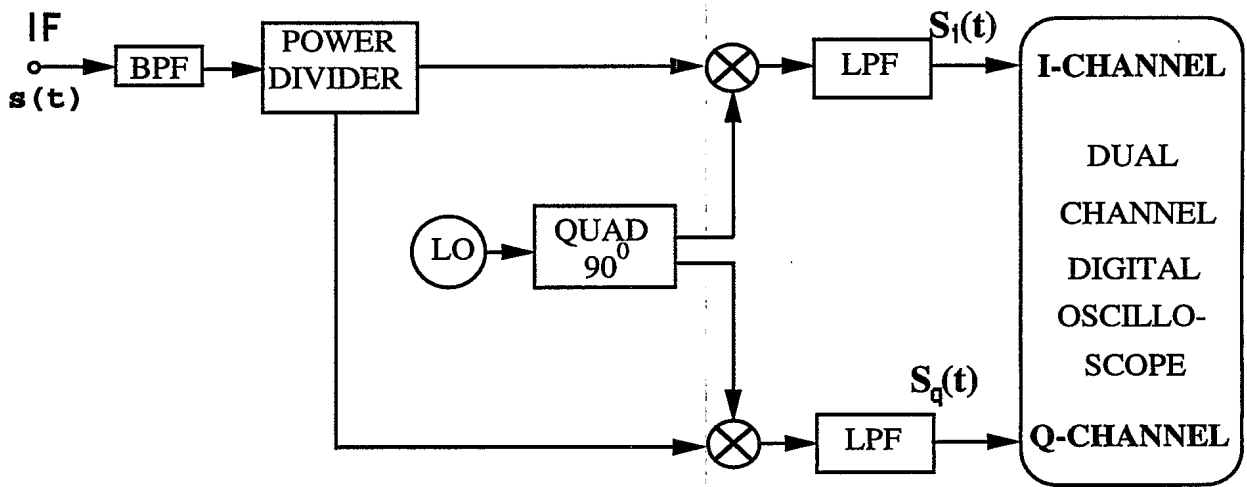


Figure 1 Block Diagram of I/Q Demodulator

In contrast to the digital approaches, there are three attractive features inherent to the conventional I/Q demodulator which can be exploited for EW applications [12-13]. They are

- (i) wide instantaneous bandwidth because the negative and positive frequencies with respect to the LO frequency can be distinguished,
- (ii) simple algorithms for the extraction of modulation characteristics can be used so that near real-time results can be obtained and
- (iii) a larger dynamic range can usually be obtained from a given A/D converter when operating at a lower sampling rate and also when the signal to be digitized is lower in frequency.

As a result, this simple I/Q demodulator is very attractive for EW applications provided the imbalances and DC offsets can be kept small.

In EW applications, a large instantaneous bandwidth is required for

- (i) the demodulation of wide-band pulse compression waveforms employing frequency modulations which can have a maximum frequency excursion in the order of hundreds of MHz [14],
- (ii) measuring very fine modulations on narrow pulses with no intentional modulations or on phase coded waveforms with very high chip rates so that distortions due to finite bandwidth can be minimized,
- (iii) relaxing the requirement for a fast cueing receiver and
- (iv) for covering a full specific frequency band, such as for the navigation radar bands, with a fixed local oscillator for the down-conversion process.

In case (iii), since the frequency of the signal is unknown, a cueing receiver with a much broader bandwidth is usually needed to measure approximately its carrier frequency before a delayed version of it can be tuned to within the frequency bandwidth of the demodulator for fine analysis. Hence a wider instantaneous bandwidth on the demodulator will alleviate the requirement for the cueing receiver to measure the signal frequency accurately and thus be able to perform the cueing function in a much shorter time. Because of these four factors, the instantaneous bandwidth of an I/Q demodulator is required to be wider than the modulation bandwidths of the individual signals of interest. On the other hand, a wide instantaneous bandwidth will increase the noise bandwidth and thus will degrade the output signal-to-noise ratio. It will also increase the probability of signal overlapping which can cause distortions. As a result, there will be an optimum bandwidth for each specific application. In EW applications, an instantaneous bandwidth of about 100 to 200 MHz is a good compromise in terms of performance and, at the same time, should be wide enough for detecting most of the signals of interest.

Commercially available quadrature mixers, are known to exhibit relatively large amplitude and phase imbalances and DC offsets [13,15] and they become worse as the operating bandwidth is increased. However, very little information is available in the open literature on the imbalances and DC offsets of wideband I/Q demodulators. In this report, we show that the imbalances and DC offsets of wideband I/Q demodulators using " off-the-shelf " components can be greatly reduced and have excellent matching characteristics. This is achieved by using the techniques of component matching and through the procedure of calibration. A DFT technique is developed to calibrate and characterize accurately wideband I/Q demodulators by using a test signal. A number of wideband I/Q demodulators are evaluated over input signal level, time and temperature and their characteristics are also reported.

## 2.0 I/Q DEMODULATORS

An incoming RF signal is usually down-converted to an IF signal before it is applied to the I/Q demodulator. The IF signal to the I/Q demodulator, as shown in Fig. 1, can be expressed in the form of

$$s(t) = a(t) \cos[\omega_o t + \phi(t)] \quad (1)$$

where  $a(t)$  is the amplitude or envelope,  $\omega_o$  is the IF angular carrier frequency and  $\phi(t)$  is the phase function of the signal. It is first bandpass filtered and then equally power-divided into two paths. The signal in each path is then mixed down to baseband by the use of a local oscillator signal. The two local oscillator signals are derived from the same source, but are 90 degrees out of phase. The resultant in-phase and quadrature baseband signals after the LPF are,

$$S_i(t) = K/2 a(t) \cos[(\omega_o - \omega_{lo})t + \phi(t) - \gamma] = K/2 a(t) \cos[\beta(t)] \quad (2)$$

and

$$S_q(t) = K/2 a(t) \sin[\beta(t)] \quad (3)$$

respectively, where  $K$  is the net gain in each path,  $\omega_{lo}$  is the angular frequency of the local oscillator with initial phase  $\gamma$ ,  $\beta(t)$  is the phase function of the baseband signal and, a constant delay introduced in each path has been neglected. In this ideal case, the two channels (paths) have been assumed to be perfectly matched in amplitude, 90 degrees out of phase, and with no DC offsets.

The instantaneous power of the envelope of the input IF signal is simply related to its in-phase and quadrature baseband components by

$$a^2(t) = 4/K^2 [S_i^2(t) + S_q^2(t)], \quad (4)$$

the signal phase function is given by

$$\begin{aligned} \phi(t) &= \beta(t) - (\omega_o - \omega_{lo})t + \gamma \\ &= \tan^{-1} [S_q(t)/S_i(t)] - (\omega_o - \omega_{lo})t + \gamma \end{aligned} \quad (5)$$

and the instantaneous frequency is

$$f_{in}(t) = \frac{d\phi(t)}{2\pi dt} = \frac{d}{2\pi dt} \left[ \tan^{-1} [S_q(t)/S_i(t)] \right] - (\omega_o - \omega_{lo})/(2\pi). \quad (6)$$

The in-phase and quadrature baseband signals are usually sampled and digitized at  $t_n = nT_s + T_o$ , where  $T_s$  is the sampling interval,  $T_o$  is the initial time and  $n = 0, 1, 2, \dots$ . In this case, the sampled instantaneous frequency is then approximately given by

$$f_{in}(t_n) \approx \left[ \phi(t_n) - \phi(t_{n-1}) \right] / (2\pi T_s). \quad (7)$$

In the implementation of the I/Q demodulator, there will be differential gain, DC offsets and phase deviation from the ideal 90 degrees between the two channels [3]. Each of which includes not just the quadrature mixer, but also the LO, LPF and the conditioning circuitry associated with the A/D converter in the digital oscilloscope. Equations (2) and (3) can then be rewritten in a more general form as

$$S_i(t) = K_i/2 a(t) \cos[\beta(t) + \phi_i] + a_{i0} \quad (8)$$

and

$$S_q(t) = K_q/2 a(t) \sin[\beta(t) + \phi_q] + a_{q0} \quad (9)$$

respectively, where  $a_{i0}$  and  $a_{q0}$  are the amplitude DC offsets,  $K_i$  and  $K_q$  are the gains, and  $\phi_i$  and  $\phi_q$  are the phase offsets of the in-phase and quadrature channels respectively. Note that  $a_{i0}$ ,  $a_{q0}$ ,  $K_i$ ,  $K_q$ ,  $\phi_i$  and  $\phi_q$  are, in general, a function of frequency.

### 3.0 CHARACTERIZATION MEASUREMENT TECHNIQUE

In this section, we will present a simple technique for characterizing the imbalances and DC offsets of wideband I/Q demodulators by using a test signal. When a test signal, of the form given by Eq.(1), is applied to the I/Q demodulator, the resultant in-phase and quadrature baseband signals are given by Eqs. (8) and (9) respectively. Expressing the baseband signal in the quadrature channel in terms of the phase imbalance ( $\phi_q - \phi_i$ ), Eq.(9) can be rewritten as

$$S_q(t) = a(t) K_q/2 \left[ \sin [\beta(t) + \phi_i] \cos[(\phi_q - \phi_i)] + \cos [\beta(t) + \phi_i] \sin[(\phi_q - \phi_i)] \right] + a_{q0} \quad (10)$$

Taking the Fourier transform of the above expression over a finite duration T, we have

$$\mathcal{F}[S_q(t)] = K_q/2 \cos[(\phi_q - \phi_i)] \mathcal{F}\left[a(t) \sin [\beta(t) + \phi_i]\right] + K_q/2 \sin[(\phi_q - \phi_i)] \mathcal{F}\left[a(t) \cos [\beta(t) + \phi_i]\right] + \mathcal{F}[a_{q0}] \quad (11)$$

$$\text{where } \mathcal{F}[h(t)] = \int_{-T/2}^{T/2} h(t) \exp(-j2\pi ft) dt \quad (12)$$

is the finite Fourier transform of  $h(t)$ . The Fourier transform of the in-phase component given by Eq. (8) is

$$\mathcal{F}[S_i(t)] = K_i/2 \mathcal{F}\left[a(t) \cos[\beta(t) + \phi_i]\right] + \mathcal{F}[a_{i0}] \quad (13)$$

If the time duration T is chosen so that there will be negligible overlapping between the frequency spectrum of the signal and the spectrum of the truncated DC offset, the DC frequency component due to the DC offset can be separated and removed. The DC offsets of the in-phase and quadrature channels are simply related to its finite Fourier transform by

$$a_{i0} = \left[ \mathcal{F}[a_{i0}] \text{ at } f = 0 \right] / T \quad (14)$$

and

$$a_{q0} = \left[ \mathcal{F}[a_{q0}] \text{ at } f = 0 \right] / T \quad (15)$$

respectively.

Since the Fourier transform provides a 2-sided spectrum, a Hilbert transform based analytic signal is needed to yield the quadrature component. For the in-phase baseband signal, the amplitude  $[K_i/2 a(t)]$  and the phase function  $[\beta(t) + \phi_i]$  as a function of instantaneous frequency can be determined by using a Hilbert transform based analytic signal  $[z_i(t)]$ , given by

$$\begin{aligned} z_i(t) &= K_i/2 a(t) \cos[\beta(t) + \phi_i] + j \mathcal{H}\{ a(t) \cos[\beta(t) + \phi_i] \} \\ &= K_i/2 a(t) \exp\{j[\beta(t) + \phi_i]\} \end{aligned} \quad (16)$$

where  $\mathcal{H}$  denotes the Hilbert transform. Note that the amplitude  $[K_i/2 a(t)]$  and the phase function  $[\beta(t) + \phi_i]$  of the in-phase calibration baseband signal may only be considered independently as expressed by Eq. (16) if the spectra of  $a(t)$  and  $\cos[\beta(t) + \phi_i]$  are separated or almost separated in frequency (that is, a narrowband signal) [16]. This is important because the amplitude and phase components must be separated and evaluated by manipulating the information in the frequency domain, at the instantaneous frequency defined by Eq. (6). If there is any significant interaction between the positive and negative spectral components associated with the phase term,  $[\beta(t) + \phi_i]$ , then the Hilbert transform will not yield the quadrature component of the input signal.

The Hilbert transform based analytic signal can be generated by first eliminating negative frequencies of the spectrum and then taking the inverse Fourier transform, given by

$$z_i(t) = 2 \int_0^{\infty} F_i(f) \exp(j2\pi ft) df \quad (17)$$

where  $F_i(f) = \mathcal{F}\{K_i/2 a(t) \cos[\beta(t) + \phi_i]\}$ , the Fourier transform of the in-phase analytic signal is simply related to  $F_i(f)$  by

$$\begin{aligned} Z_i(f) &= \mathcal{F}[z_i(t)] = 2 F_i(f) U(f) = \begin{cases} 2F_i(f) & f > 0 \\ 0 & f < 0 \end{cases} \\ &= K_i/2 \mathcal{F}\left[ a(t) \exp\{j[\beta(t) + \phi_i]\} \right] \end{aligned} \quad (18)$$

Similarly, using Eq. (11) the Fourier transform of the quadrature analytic signal is

$$Z_q(f) = -j K_q/2 \exp[j(\phi_q - \phi_i)] \mathcal{F}\left[ a(t) \exp\{j[\beta(t) + \phi_i]\} \right] \quad (19)$$

Taking the ratio of the Hilbert transform on the analytic signal  $[z_q(t)]$  in the quadrature channel to the one  $[z_i(t)]$  in the in-phase channel, we have

$$Z_q(f)/Z_i(f) = R \exp\left[j[(\phi_q - \phi_i) - \pi/2]\right] \quad (20)$$

If there is no overlapping between the amplitude and phase functions in the frequency domain, the ratio of  $Z_q(f)/Z_i(f)$ , as a function of frequency, can be computed at each frequency. As a result, the relative amplitude imbalance ratio  $R$  ( $K_q/K_i$ ) and the phase imbalance  $(\phi_q - \phi_i)$ , as a function of instantaneous frequency, can then be determined. Using the above procedure and knowing the input IF frequency, the imbalance errors and DC offsets of the demodulator, as a function of frequency, can thus be measured.

In practice, the baseband signals are sampled and digitized. As a result, a discrete Fourier transform (DFT) has to be used with  $t$  replaced by  $t_n$ . As stated above, any signal classified as narrow-band can be used as a test signal. However, a CW calibration signal usually is used for two main reasons: (i) precise CW sources are readily available and (ii) the number of data samples generated at a specific frequency of interest can be made arbitrarily large. A large number of data samples for the DFT can improve the output signal-to-noise ratio, and thus, the ultimate accuracy of the measurement. Since both the input IF frequency and the resultant baseband frequency are known, the number of sample points can also be chosen to satisfy the criterion of having a truncation interval for the DFT equal to an integer multiple of the period of the baseband signal. Once this criterion is satisfied, the leakage problem due to time domain truncation associated with DFT can be eliminated [17]. As a result, no distortions are introduced to either the CW signal or the DC offset. The DC offset is determined by dividing the DC component of the DFT by the total number of sample points ( $N$ ) used.

The approach taken in this report for measuring the imbalance errors and DC offsets is slightly different from the one given by F.E. Churchill, G.W. Ogar and B.J. Thompson [5]. In Reference 5, the application is for radar receivers where the bandwidth is narrow and a single calibration measurement at about the center band of the receiver is sufficient, while here, the bandwidth is much larger and the calibration measurement may be needed throughout the whole frequency band. As a result, the approach of taking exactly  $N$  samples over one cycle of the baseband calibration signal as given in Reference 5 can not be applied to some of the calibration frequencies in this application. The only requirement is to increase the number of samples,  $N$ , for the DFT so that the number of sample points chosen satisfy the criterion of having a truncation interval for the DFT equal to an integer multiple of the period of the baseband calibration signal. Once this criterion is satisfied, the leakage problem due to time domain truncation associated with the DFT can be eliminated.

This leakage problem is illustrated in Fig. 2. with a total number of sample points for the DFT equal to 100 with a calibration point located at every  $\delta f/f_s = 0.01$  interval, where  $f_s = 1/T_s$ . 100 samples are needed to satisfy the criterion of having a truncation interval equal to an integer multiple of the period of the baseband calibration signal at all calibration points. Figure 2 illustrates the effect when the number of samples differs from 100 and they are plotted for  $N$  equals 99, 100 and 101. When the total number of sampling points is other than 100, leakage will occur at each calibration frequency point and the error introduced will be a function of the signal frequency in terms of its normalized frequency location as well as the deviation between the signal frequency and its DFT frequency for a given number of sample

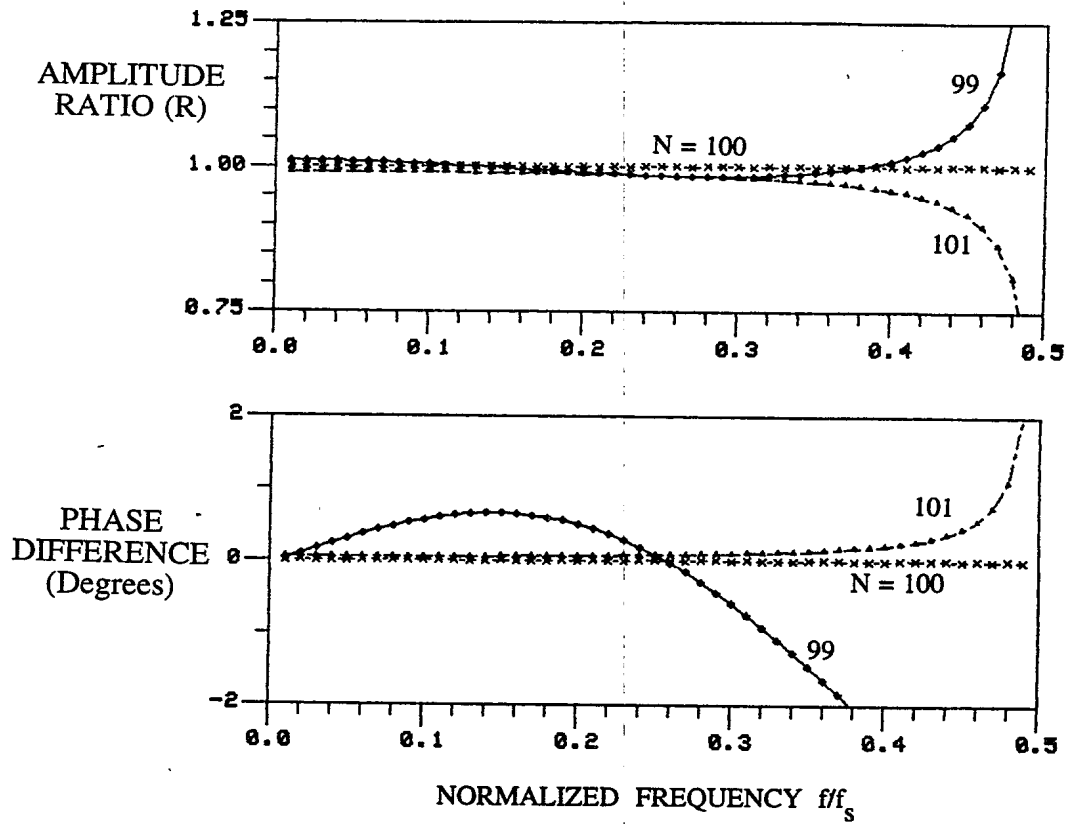


Figure 2 Computed Phase Deviation and Amplitude Ratio due to Leakage

points. In this report, the frequency and sampling rates are assumed to be exact, and as a result, no frequency deviations are introduced. The leakage effect can also be reduced by using windowing [17]. However, the resultant broadening effect on the spectrum may cause significant interaction between the positive and negative spectral components associated with the phase term at both the low and high ends of the spectrum.

Another deviation from the methodology of Reference 5 is that a DFT is performed separately on the data from the two channels. A relative comparison of the two DFTs is then carried out to determine the imbalance errors. In Reference 5, the data from the two channels are combined into a complex expression and a DFT is taken and expressed in terms of the test signal frequency and its image frequency.

#### 4.0 MATCHING CHARACTERISTICS OF WIDEBAND I/Q DEMODULATORS

Implementation of the I/Q demodulator is carried out by the use of a quadrature mixer, a local oscillator and a dual-channel digital oscilloscope. The quadrature mixers tested are " off-the-shelf " units from both Anaren Microwave Inc., and KDI/Triangle Electronics Inc., and custom-matched quadrature mixers composed of discrete components. The digital oscilloscopes are either the 10-bit 9430 or 8-bit 9450 dual-channel oscilloscope from LeCroy Corporation. On any given set of measurements, the set-up is usually turned on for at least 20 minutes before the testing begins. Depending on the type of testing, the actual time taken to complete the test typically can last over a period of minutes. As a result, if the characteristics of the I/Q demodulator vary as a function of time, their changes are also reflected in the experimental data.

The " off-the-shelf " quadrature mixers are found to have relatively larger imbalances and DC offsets when compared to the custom-matched devices. Two custom-matched devices and a quadrature mixer from Anaren Microwave Inc. are fully tested as a function of input power level and are given in this report. The I/Q demodulators using these quadrature mixers are tested over 100-MHz and 200-MHz bandwidths. They are also tested over time and temperature. No attempt is made to fully analyze the imbalances and DC offsets on any particular component in the demodulator as the demodulator is tested as a subsystem.

##### 4.1 Imbalances and DC Offsets Over a Range of Input Signal Power Level

The imbalances and DC offsets of I/Q demodulators are measured by using the technique described in Section 3.0. The I/Q demodulator chain includes a quadrature mixer, a 3-dB pad, an interconnecting cable and a LeCroy dual-channel digital oscilloscope. The 3-dB pad is used to improve the impedance matching between the quadrature mixer and the oscilloscope. The in-phase and quadrature signals are sampled and digitized by the oscilloscope. The I/Q demodulators are tested as a function of LO power level and input signal frequency and power level. A CW signal from a frequency synthesizer is used as a test signal to characterize the I/Q demodulator.

The test results on the I/Q demodulators using custom-matched quadrature mixers are discussed in detailed in this section. In general, the custom-matched quadrature mixers units ( A and B ), as shown in Fig 3, have better matching characteristics because the discrete components can be individually selected and matched by inserting either an isolator or attenuator, adapters and/or line stretchers. A line stretcher is inserted in one of the outputs of



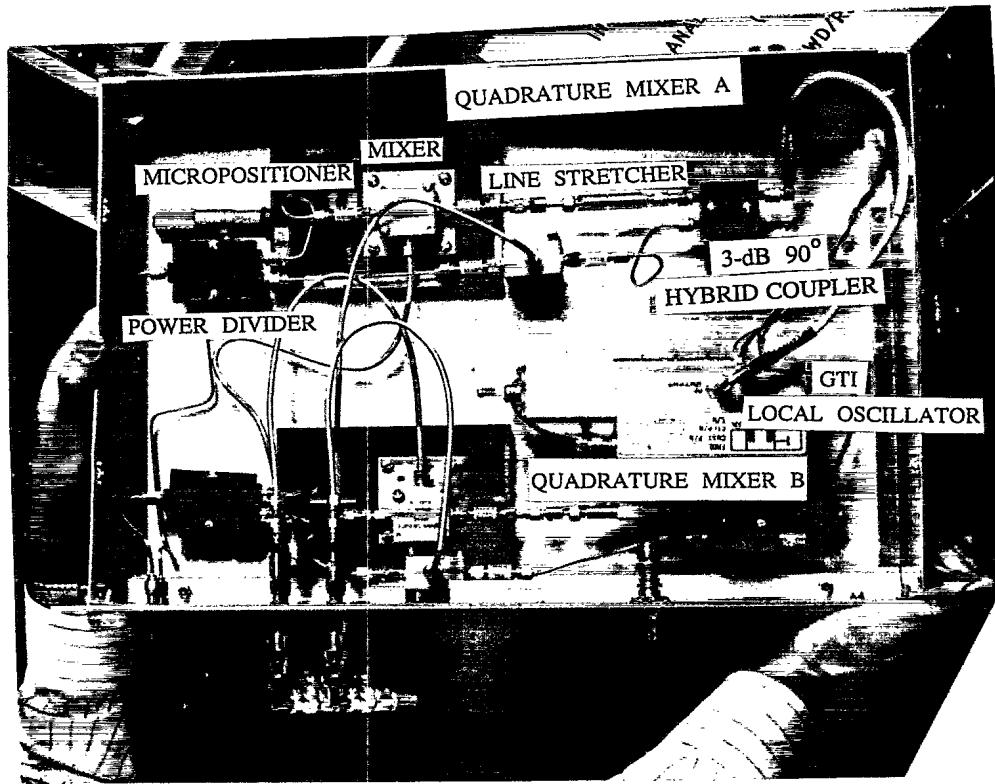


Figure 3 Quadrature Mixers A and B



the quadrature power divider of the LO subassembly as shown in the figure. The length of the line-stretcher is adjustable through a micrometer and then locked in place. The LO is a synthesizer from Communication Techniques Inc. with an output frequency of 1 GHz. The line stretcher is first adjusted so that the in-phase and quadrature signals are 90 degrees out of phase close to zero baseband frequency, and then coarse testing is carried out to characterize the I/Q demodulator as a function of frequency. If there is any residual mismatch in terms of cable lengths between the in-phase and quadrature channels, a linear slope will appear on the phase imbalance plot as a function of frequency. This linear slope is then reduced by inserting a small section of cable at the output of either the in-phase or quadrature channels. The extra cable length is implemented by using off-the-shelf adapters with various lengths. After the coarse adjustment is made, then a comprehensive testing is carried out.

In the first set of measurements, the input signal power level is adjusted so that close to full scale deflection is achieved on the digital oscilloscope when it is set at 10 mV/division. The same input power level is maintained as the signal frequency is varied by 4 MHz steps. At each input signal frequency, a 10,000-point DFT is performed on the digitized baseband signal to extract the relative amplitude and phase difference between the two channels and the DC offset in each channel. A typical SNR of approximately 48 dB is achieved on each sample. When a DFT is performed on 10,000 sample points, the SNR is approximately improved by an additional factor of 40 dB. As a result, the combined output SNR is approximately 88 dB. The noise distribution is approximately Gaussian and the errors introduced by the noise [13] are small enough that their effects on the measurements can be neglected.

Another eight sets of measurements are then taken by reducing the input power level by 3 dB steps. At the lowest input signal level, the combined output SNR is approximately 64 dB which gives an estimated RMS phase error due to noise of less than 0.05 degrees. The nine sets of measurements are analyzed to compute the imbalance errors and DC offsets of the I/Q demodulator at each frequency.

#### 4.1.1 100-MHz Demodulators

The two custom-matched quadrature mixers (units A and B), as shown in Fig.3, are tested in the laboratory with a 10-bit LeCroy 9430 dual-channel digital oscilloscope. The LO power applied to the input of the quadrature mixer is set at 19 dBm. The in-phase and quadrature signals are sampled and digitized by the oscilloscope at a 100-MHz sampling rate with a low-pass filter bandwidth of approximately 150 MHz. A CW signal from a frequency synthesizer is applied to the input of the I/Q demodulator and is then adjusted in frequency to produce a baseband signal over the range from - 50 MHz to 50 MHz.

The means of the imbalances and DC offsets are plotted in Fig. 4 and are indicated by a solid line. There are twenty four experimental points in each set of measurements and its location along the frequency axis is indicated by a small circle. The statistics on the matching characteristics are summarized in Table I. Column 1 gives the RMS error from an ideal I/Q demodulator over the full baseband frequency range of  $\pm 50$  MHz and a 24-dB dynamic range. It represents the worst case error when there is no correction. Column 2 gives the mean value of each characteristic over the full frequency range of  $\pm 50$  MHz and a 24-dB dynamic range. The RMS error when this mean is subtracted from the measurement is given in Column 3. In order to provide another indicator on whether there is an offset introduced on the imbalances and DC offsets at each input power level, the mean value for each frequency is computed and then subtracted before the RMS value is computed. The revised RMS value is enclosed in

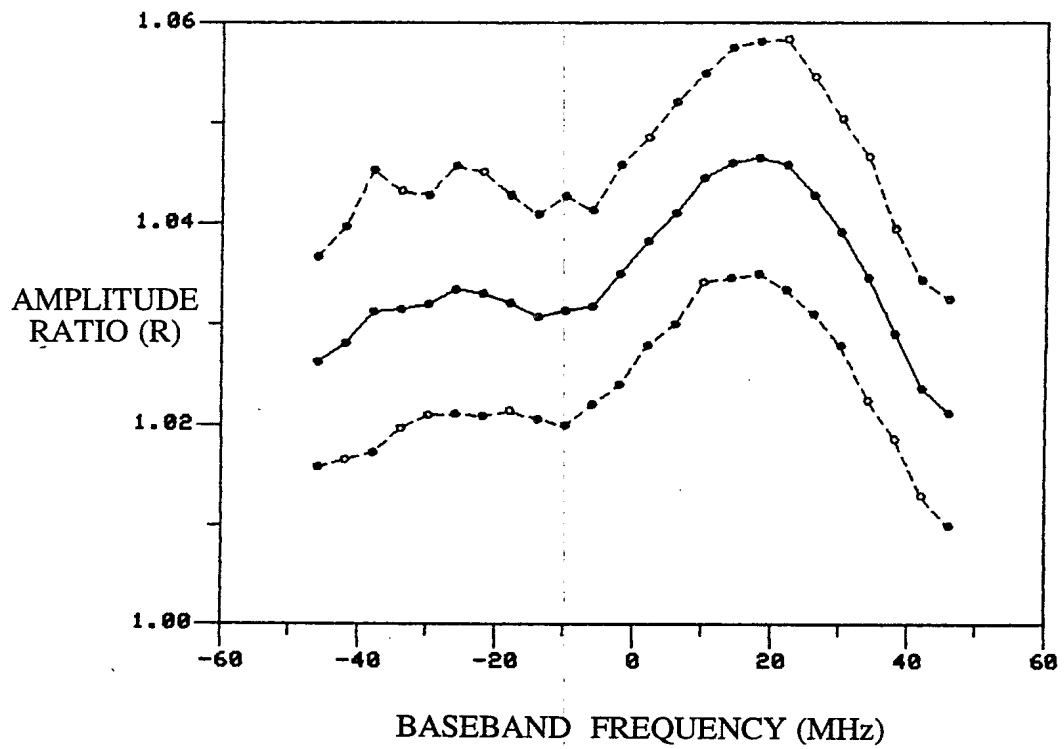


Figure 4(a) Amplitude Ratio Versus Baseband Frequency of Quadrature Mixer B with 10-bit Oscilloscope over a 24-dB Dynamic Range and 100 MHz-Bandwidth (10 mV/D)

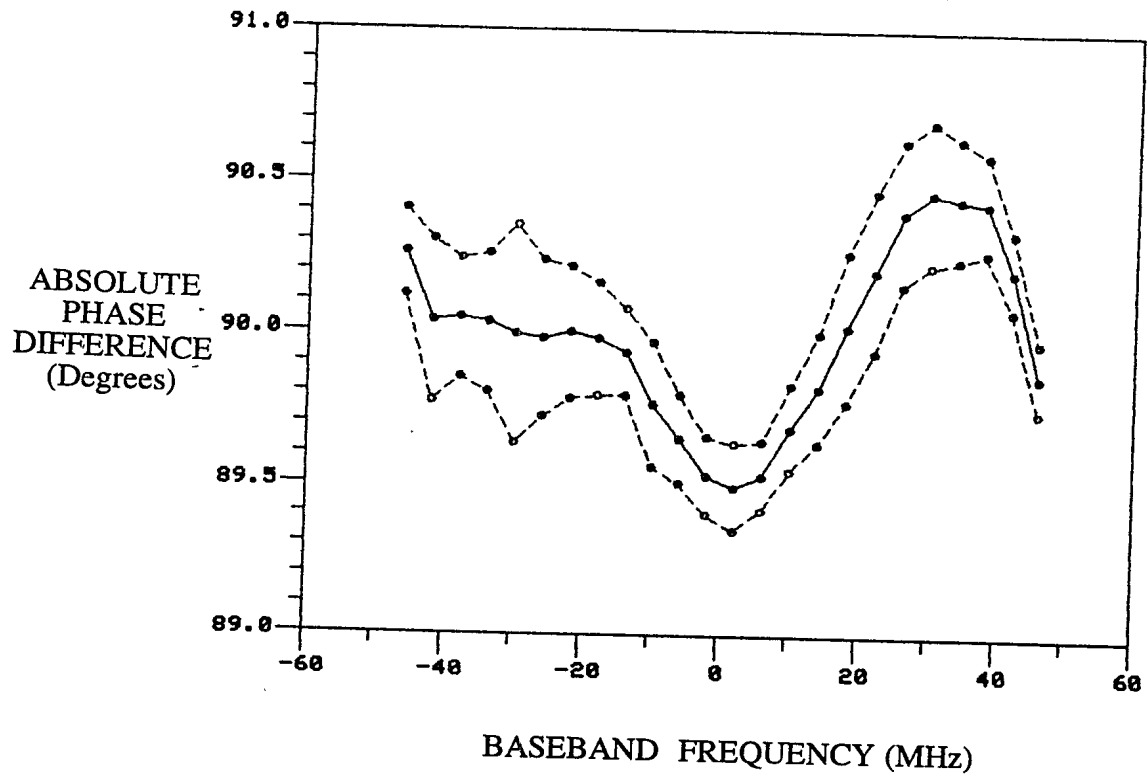


Figure 4(b) Absolute Phase Difference Versus Baseband Frequency of Quadrature Mixer B with 10-bit Oscilloscope over a 24-dB Dynamic Range and 100 MHz-Bandwidth (10 mV/D)

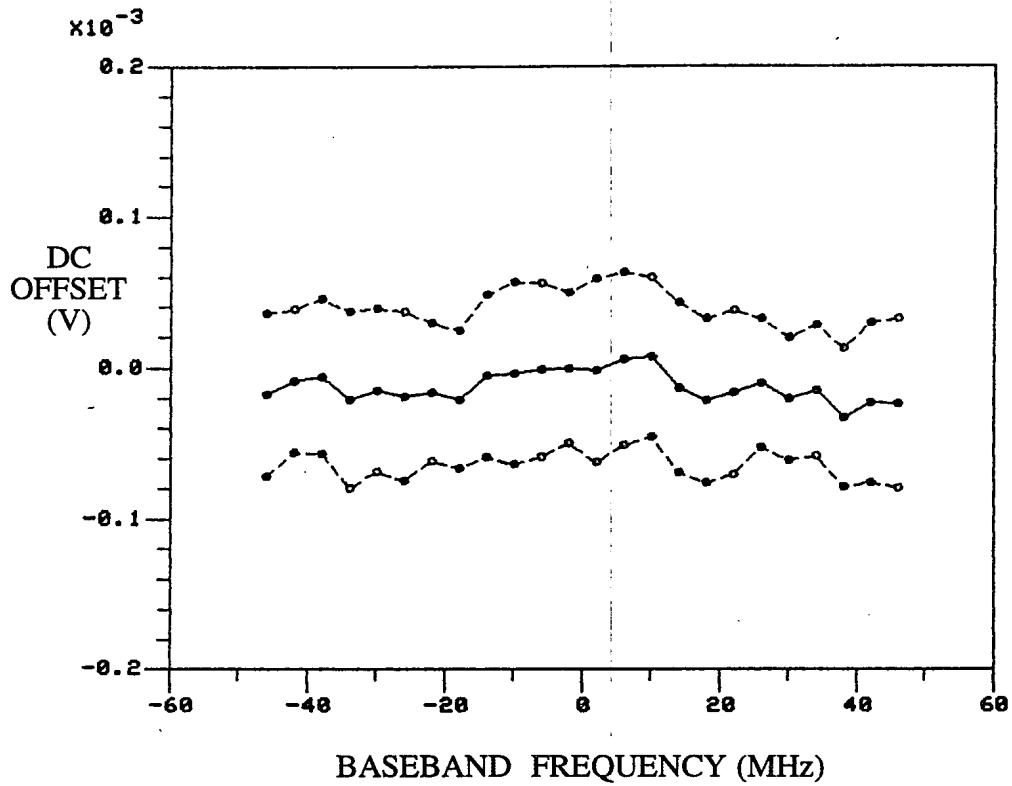


Figure 4(c) DC Offset Versus Baseband Frequency (In-phase Channel) of Quadrature Mixer B with 10-bit Oscilloscope over a 24-dB Dynamic Range and 100 MHz-Bandwidth (10 mV/D)

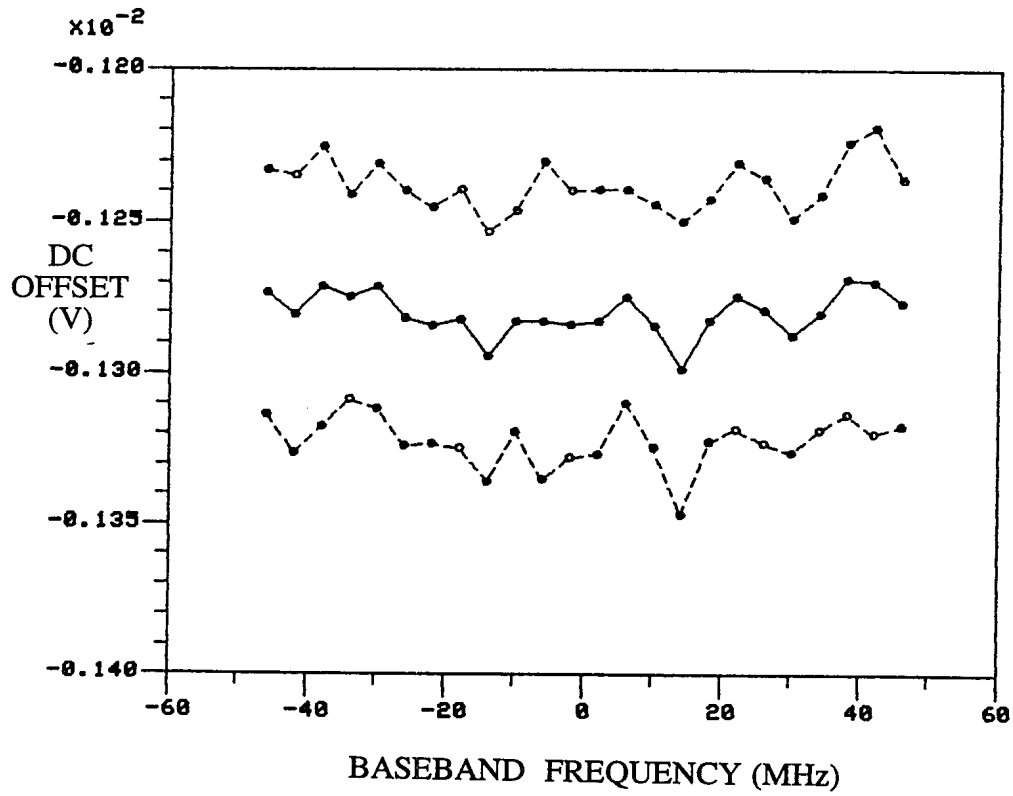


Figure 4(d) DC Offset Versus Baseband Frequency (Quadrature Channel) of Quadrature Mixer B with 10-bit Oscilloscope over a 24-dB Dynamic Range and 100 MHz-Bandwidth (10 mV/D)

braces in the last column of the Table.

Table I

Imbalances and DC Offsets of Quadrature Mixer B with 10-bit Oscilloscope over a 24-dB Dynamic Range and 100 MHz-Bandwidth (10 mV/D)

	RMS Error from Ideal Demodulator	Mean	RMS error with Mean Subtracted
Amplitude	0.0369 (0.643 dB)	1.035 (0.295 dB)	0.0133 (0.0072)
Phase	0.348°	89.991°	0.348° (0.342°)
DC Offsets			
In-phase	0.055 mV	-0.013 mV	0.053 mV (0.022 mV)
Quadrature	1.281 mV	-1.280 mV	0.043 mV (0.019 mV)

The mean, (mean + RMS) and (mean - RMS) of the amplitude ratio  $R$  versus baseband frequency are plotted in Fig. 4 (a). The mean amplitude ratio over the full baseband frequency range of  $\pm 50$  MHz and a 24-dB dynamic range is computed to be 1.035 (0.295 dB) and given in Table I. The RMS value from the mean is 0.0133 and when expressed in terms of  $20 \cdot \log_{10} [( \text{mean} + \text{RMS}) / (\text{mean} - \text{RMS})]$ , it is 0.223 dB. If the RMS value is measured from the ideal value of unity, then it is .0369 or 0.643 dB. If the mean at each input power level is subtracted before the RMS value is computed, it is reduced to 0.0072.

The absolute phase difference between the quadrature channel and the in-phase channel is plotted in Fig. 4 (b). The RMS value of the phase difference from the ideal quadrature is 0.348 degrees. The mean value over the full baseband frequency range of  $\pm 50$  MHz and a 24-dB dynamic range is 89.991 degrees. If the mean is subtracted, then the RMS value is also 0.348 degrees. If the mean value at each input signal power level is computed and then subtracted before the RMS value is computed for each frequency, the revised RMS value is almost unchanged at 0.342 degrees.

The DC offsets in millivolts of both the in-phase and quadrature channels are plotted in Figs. 4 (c) and 4(d) respectively. The RMS DC offsets in the in-phase and quadrature channels are 0.055 mV and 1.281 mV respectively. The mean DC offset values of the in-phase and quadrature channels are -0.013 mV and -1.280 mV respectively. After the mean is subtracted, the RMS values for both the in-phase and quadrature channels are 0.053 mV and 0.043 mV respectively over the baseband frequency range of  $\pm 50$  MHz and a 24-dB dynamic range. If the mean value at each input signal power level is subtracted first before the RMS value is computed, then the in-phase and quadrature RMS DC offsets are reduced approximately by a factor of 2 to 0.022 mV and 0.019 mV respectively.

After the mean value is subtracted from the imbalance errors and DC offsets, the residual errors are very small and are approaching the residual errors due to noise alone.

The dynamic range of the demodulator can be increased by adjusting the oscilloscope voltage setting. A similar test is carried out by changing the oscilloscope setting from 10 mV/D to 5 mV/D. The only change in the hardware is the last section of the demodulator and as expected there are similar characteristics between the two sets of curves. The characteristics on this new setting are tabulated in Table II. The phase error is slightly worse while the DC offsets are better.

Table II

Imbalances and DC Offsets of Quadrature Mixer B with 10-bit Oscilloscope over a 24-dB Dynamic Range and 100 MHz-Bandwidth (5 mV/D)

	RMS Error from Ideal Demodulator	Mean	RMS error with Mean Subtracted
Amplitude	0.0285 (0.496 dB)	1.027 (0.231 dB)	0.0095 (0.0088)
Phase	0.525°	89.940°	0.522° (0.521°)
DC Offsets			
In-phase	0.033 mV	-0.016 mV	0.029 mV (0.023 mV)
Quadrature	1.257 mV	-1.257 mV	0.029 mV (0.022 mV)

Another similar quadrature mixer (A) with the same oscilloscope is also tested and a summary of the results for oscilloscope setting at 10 mV/D and 5 mV/D are given in Tables III and IV respectively. I/Q demodulator A in general has better amplitude and phase matching characteristics than I/Q demodulator B. However, the mean in-phase DC offset in the I/Q demodulator A is much higher and its RMS value is much worse at the 10 mV/D range. The main problem is due to large mean DC offsets introduced by the in-phase mixer at the two strongest signal levels of the test. If these two data points are removed in the computation, the resultant RMS in-phase DC offset value is much smaller.

Table III

Imbalances and DC Offsets of Quadrature Mixer A with 10-bit Oscilloscope over a 24-dB Dynamic Range and 100 MHz-Bandwidth (10 mV/D)

	RMS Error from Ideal Demodulator	Mean	RMS error with Mean Subtracted
Amplitude	0.0476 (0.828 dB)	1.047 (0.401 dB)	0.0060 (0.0045)
Phase	0.328°	90.066°	0.321°(0.320°)
DC Offsets			
In-phase	0.778 mV	0.751 mV	0.204 mV (0.030 mV)
Quadrature	0.523 mV	0.522 mV	0.030 mV (0.026 mV)

Table IV

Imbalances and DC Offsets of Quadrature Mixer A with 10-bit Oscilloscope over a 24-dB Dynamic Range and 100 MHz-Bandwidth (5 mV/D)

	RMS Error from Ideal Demodulator	Mean	RMS error with Mean Subtracted
Amplitude	0.0474 (0.820 dB)	1.047 (0.396 dB)	0.0087 (0.0045)
Phase	0.264°	90.094°	0.247°(0.246°)
DC Offsets			
In-phase	0.866 mV	0.864 mV	0.070 mV (0.028 mV)
Quadrature	0.539 mV	0.538 mV	0.032 mV (0.025 mV)

With the same set-up, the above sets of measurements are repeated three days later in the laboratory. The purpose of this test is to evaluate the stability of the imbalance errors and DC offsets of the I/Q demodulator over time. The results indicate that there are negligible differences in the imbalance errors and DC offsets over a period of three days.

In general, the imbalances and DC offsets with the mean removed are quite small with the exception of the in-phase DC offset of quadrature mixer A operating at 10 mV/D. From Tables I, II and IV, the combined RMS amplitude imbalance with the mean subtracted is .017 while the phase imbalance is 0.389 degrees. This will give an image rejection ratio of - 40.9 dB. The RMS DC offset from Table I on both the in-phase and quadrature channels is 0.048 mV. When it is normalized by the total amplitude range of 80 mV, we have a ratio of

- 64.4 dB. The RMS DC offset of both the in-phase and quadrature channels from Tables II and IV is 0.043 mV. When it is normalized by the total amplitude range of 40 mV, a ratio of -59.3 dB is obtained.

#### 4.1.2 200-MHz Demodulators

The imbalances and DC offsets of quadrature mixers A, B and one " off-the-shelf " quadrature mixer from Anaren Microwave Inc. are tested again over a wider bandwidth eight months later. In these sets of measurements, the testing is carried out in a radar signal collection shelter where there is little control over temperature. The set-up of the quadrature mixers used for this set of measurements are slightly modified and different from Section 4.1.2. The LO power is lower, and different cable lengths and slightly different input signal power levels are used. The total time taken to complete each test is about 7 minutes.

I/Q demodulator A is tested using the 10-bit oscilloscope set at 10 mV/D. The baseband frequency range is from - 117 MHz to 118 MHz at 5-MHz steps. The bandwidth of the analog LPF of the oscilloscope is about 150 MHz. The imbalances and DC offsets at frequencies higher than the Nyquist frequency are obtained by processing data at the aliased frequency. A summary of the imbalances and DC offsets are tabulated in Table V. When these characteristics are compared to those with a 100-MHz bandwidth, a slight degradation is noticed as expected.

Table V

Imbalances and DC Offsets of Quadrature Mixer A with 10-bit Oscilloscope over a 24-dB Dynamic Range and 235 MHz-Bandwidth (10 mV/D)

	RMS Error from Ideal Demodulator	Mean	RMS error with Mean Subtracted
Amplitude	0.0575 (0.999 dB)	1.057 (0.477 dB)	0.0102 (0.0098)
Phase	0.752°	90.206°	0.723°(0.578°)
DC Offsets			
In-phase	0.698 mV	0.664 mV	0.214 mV (0.073 mV)
Quadrature	0.338 mV	0.336 mV	0.032 mV (0.029 mV)

Another set of measurements is taken on quadrature mixer B sampled at 400 MHz using the 8-bit oscilloscope. A pair of 4-section Bessel LPFs with differential group delays of less than 0.65 ns over the passband of 120 MHz are used. The baseband frequency range is from -101 MHz to 99 MHz with a frequency step size of 4 MHz. The resultant characteristics are summarized in Table VI.

Table VI

Imbalances and DC Offsets of Quadrature Mixer B with 8-bit Oscilloscope over a 24-dB Dynamic Range and 200 MHz-Bandwidth (10 mV/D)

	RMS Error from Ideal Demodulator	Mean	RMS error with Mean Subtracted
Amplitude	0.0588 (1.023 dB)	1.055 (0.466 dB)	0.0205 (0.0191)
Phase	1.056°	90.105°	1.051°(1.047°)
DC Offsets			
In-phase	0.462 mV	-0.457 mV	0.070 mV (0.060 mV)
Quadrature	1.499 mV	-1.498 mV	0.067 mV (0.055 mV)

Using a similar set-up as above except with the quadrature mixer B replaced by an Anaren 210 quadrature mixer. The extra phase imbalance from this device is compensated using cables and adapters placed in the baseband ports. The resultant characteristics are summarized in Table VII.

Table VII

Imbalances and DC Offsets of Anaren 210 Quadrature Mixer with 8-bit Oscilloscope over a 24-dB Dynamic Range and 200 MHz-Bandwidth (10 mV/D)

	RMS Error from Ideal Demodulator	Mean	RMS error with Mean Subtracted
Amplitude	0.0430 (0.748 dB)	1.036 (0.307 dB)	0.0240 (0.0227)
Phase	1.604°	90.988°	1.264°(1.267°)
DC Offsets			
In-phase	14.415 mV	14.414 mV	0.213 mV (0.101 mV)
Quadrature	12.904 mV	12.902 mV	0.221 mV (0.116 mV)

Comparing the custom-matched device (quadrature mixer B ) to the Anaren quadrature mixer, the custom one has almost the same characteristics except with much better RMS DC offsets, which are about 3 times smaller for both the in-phase and quadrature channels.

#### 4.2 Imbalances and DC Offsets Over Time and Temperature

This test is also carried out in the radar signal collection facility. Quadrature mixer A is measured at a fixed input power level over the same  $\pm 50$  MHz range repeatedly as a function of time. The time needed to complete a set of measurement is about 25 seconds and the set of measurement is repeated every five minutes. Seven sets of measurements are carried out over a period of 30 minutes. The input signal power is set at a level where 90% full scale deflection is achieved on the 10 mV/D range. Note that this set up is slightly different from the one used earlier in Section 4.1.2 and taken at a different time with some adjustments made to the demodulator. The variations on the amplitude and phase mismatches, and DC offsets as a function of time are tabulated in Table VIII.

Table VIII

Imbalances and DC Offsets of Quadrature Mixer A with 10-bit Oscilloscope as a Function of Time over a Period of 30 Minutes

	RMS Error from Ideal Demodulator	Mean	RMS error with Mean Subtracted
Amplitude	0.0379 (0.658 dB)	1.038 (0.322 dB)	0.0031 (0.0030)
Phase	0.148°	89.965°	0.144°(0.143°)
DC Offsets			
In-phase	0.736 mV	0.732 mV	0.082 mV (0.036 mV)
Quadrature	0.658 mV	0.657 mV	0.023 mV (0.017 mV)

The ambient temperature was about 16 degrees C with a variation over this period of about 1 to 2 degrees. In order to compute the tracking characteristics over the whole bandwidth as a function of time, the mean value from each set of data is subtracted before the RMS calculation is performed. As can be seen from the Table, the resultant RMS phase error is almost unchanged for both the phase and amplitude. The phase RMS value is changed from 0.144 degrees to 0.143 degrees while the RMS amplitude value is from 0.0031 to 0.0030. The RMS DC offsets for the in-phase and quadrature channels are from 0.082 mV to 0.036 mV and from 0.023 mV to 0.017 mV respectively. As a result, the imbalance mismatches are negligible while there are slight DC offset shifts.

As mentioned in Section 4.1.1, similar measurements over a longer period of time in terms of days were performed in the laboratory. The variations were observed to be smaller as the temperature inside the laboratory was much more stable.

Another set of measurement was carried out over a much larger temperature range and over the course of 5 hours. The mean temperature was about 29 degrees C and the total temperature change was about 10 degrees. Six sets of measurements were taken at the 10 mV/D range with the results tabulated in Table IX.

Table IX

Imbalances and DC Offsets of Quadrature Mixer A with 10-bit Oscilloscope as a Function of Time over a Period of 5 Hours

	RMS Error from Ideal Demodulator	Mean	RMS error with Mean Subtracted
Amplitude	0.0394 (0.685 dB)	1.039 (0.332 dB)	0.0054 (0.0025)
Phase	0.865°	89.782°	0.837° (0.129°)
DC Offsets			
In-phase	0.433 mV	0.433 mV	0.0511 mV (0.031 mV)
Quadrature	0.261 mV	0.258 mV	0.036 mV (0.024 mV)

By comparing the results in Table VIII and Table IX, in general, for a bigger temperature change, there will be larger offsets introduced to the imbalances and DC offsets. If the offsets are measured and corrected frequently, small residual imbalances and DC offsets can be maintained.

Under different operating conditions, the imbalance errors and DC offsets of I/Q demodulators have also been evaluated. It is found that the imbalance errors and DC offsets are a strong function of the LO frequency and LO power level to the quadrature mixer. For I/Q A, the phase imbalance is found to vary as much as 0.8 degrees over a 4 dB change in LO power, while for the Anaren quadrature mixer, the phase change is only 0.3 degrees. Once the optimum operating LO power level and the ambient temperature are stabilized, the imbalance errors and DC offsets are found to remain extremely stable.

## 5.0 COMPENSATION THROUGH CALIBRATION

As can be seen from the results on practical I/Q demodulators, the imbalances and DC offsets can be small, if component matching is used in the design of the I/Q demodulators. The imbalances and DC offsets are very stable and small over a wide range of dynamic range and frequency. However, they are susceptible to change if there is a wide range of temperature change.

Once the imbalances and DC offsets, as a function of frequency, are known, the errors can be eliminated through a calibration. In the simplest case where the imbalance errors and DC offsets of the I/Q demodulator over the signal bandwidth are approximately constant, a single set of calibration values can be applied to every data point once the approximate

frequency of the signal is estimated. If further reduction in the systematic errors is required, a more elaborate calibration may be needed as a function of signal frequency and may be even the signal power. The ultimate acceptable imbalances and DC offsets depend on the specific application.

Once the imbalances  $[R, (\phi_q - \phi_i)]$  and DC offsets  $[a_{i0}, a_{q0}]$  are known through the calibration procedure, the next step is to compute the corrected phase function  $[\beta(t) + \phi_i]$  of the baseband signal. For this we need expressions for  $a(t) \sin[\beta(t) + \phi_i]$  and  $a(t) \cos[\beta(t) + \phi_i]$ . Using both Eqs.(8) and (9),  $a(t) \sin[\beta(t) + \phi_i]$  can be expressed in terms of the measured baseband signals, and the imbalance errors and DC offsets as

$$a(t) \sin[\beta(t) + \phi_i] = \left[ [S_q(t) - a_{q0}]/(K_q/2) - [S_i(t) - a_{i0}]/(K_i/2) \right] \cdot \sin[(\phi_q - \phi_i)] / \cos[(\phi_q - \phi_i)] \quad (21)$$

Similarly, from Eq.(8), we also have

$$a(t) \cos[\beta(t) + \phi_i] = [S_i(t) - a_{i0}]/(K_i/2) \quad (22)$$

Dividing Eq.(21) by Eq.(22) and taking the arctangent of the ratio, the phase function of the corrected baseband signal is given by

$$\begin{aligned} [\beta(t) + \phi_i] &= \alpha_o(t) \\ &= \tan^{-1} \left\{ \frac{[S_q(t) - a_{q0}]/R - [S_i(t) - a_{i0}] \sin[(\phi_q - \phi_i)]}{\cos[(\phi_q - \phi_i)][S_i(t) - a_{i0}]} \right\} \quad (23) \end{aligned}$$

Since the corrected phase function of the baseband signal is known, the corrected amplitude of the envelope is obtained by using Eq.(8). Hence

$$a(t) = 2/K_i [S_i(t) - a_{i0}]/\cos[\beta(t) + \phi_i]. \quad (24)$$

A functional block diagram showing the correction and computation procedure is given in Fig. 5.

## 6.0 SUMMARY AND CONCLUSIONS

In this report, a simple DFT technique has been developed for the characterization of imbalances and DC offsets of wideband I/Q demodulators by using a test signal. It has also been shown that the imbalances and DC offsets of wideband I/Q demodulators using "off-the-shelf" components can be greatly reduced and have excellent matching characteristics. This is achieved by using the techniques of component matching and through the procedure of calibration.

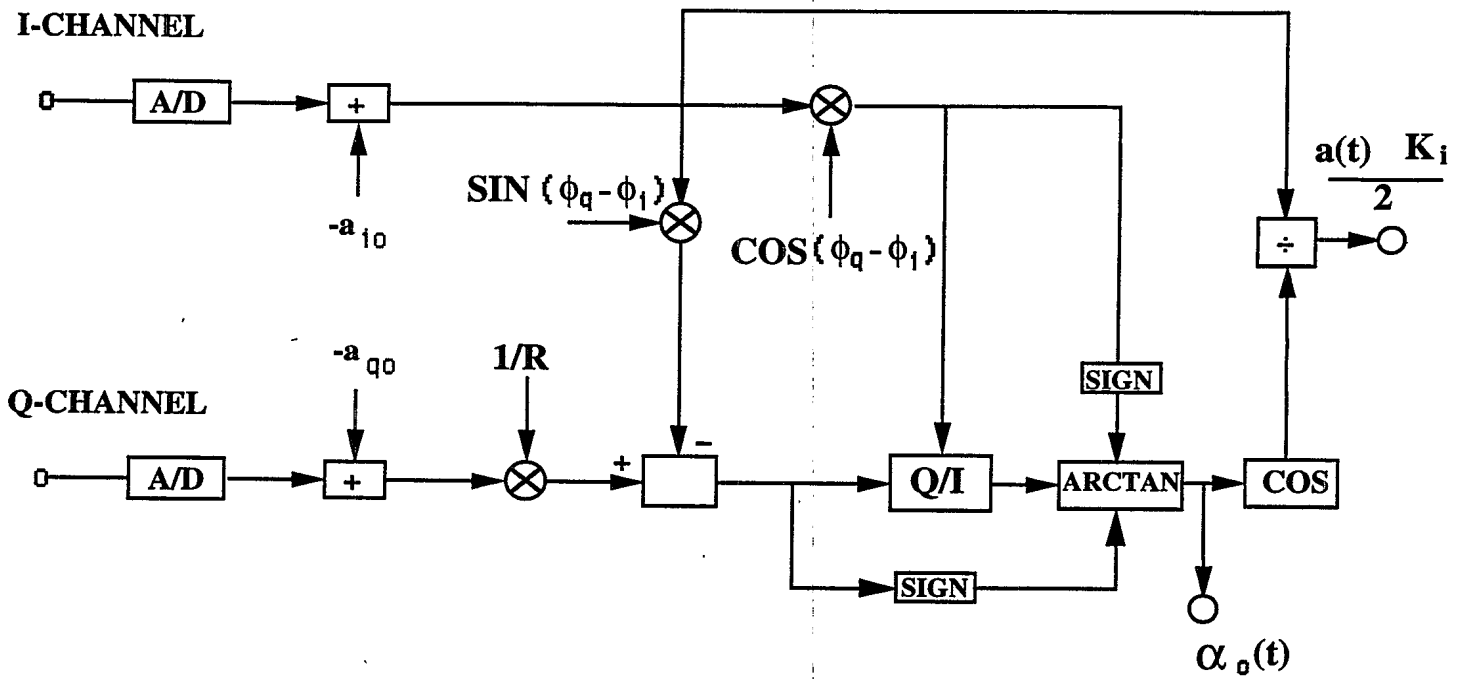


Figure 5 Functional Block Diagram of Compensation and Computation

The imbalance errors and DC offsets of wideband I/Q demodulators over a large input power dynamic range can be made small. RMS amplitude and phase imbalance errors of .017 and 0.389 degrees respectively can be achieved over an instantaneous bandwidth of 100 MHz and a dynamic range of 24 dB. The imbalance errors and DC offsets can be reduced further by calibration as a function of frequency. A number of wideband I/Q demodulators have been evaluated over input signal level, time and temperature and their characteristics are also reported.

## 7.0 REFERENCES

- [1] Tsui, J.B.Y., *Digital Microwave Receivers*, 1989, Norwood, MA: Artech House.
- [2] Skolnik, M.I., *Introduction to Radar Systems*, 2nd Edition, 1980 New York, McGraw-Hill Book Company
- [3] Goldman, S.J., " Understanding the Limits of Quadrature Detection", *Microwave & RF*, pp. 67-70, Dec 1986.
- [4] Roome, S.J., " Analysis of Quadrature Detectors using Complex Envelope Notation", In IEE proceedings, Vol. 136, Pt. F, No.2, April 1989.
- [5] Churchill, F.E., Ogar, G.W. and Thompson, B.J., " The Correction of I and Q Errors in a Coherent Processor ", In IEEE Trans. AES, Vol. AES-17, No. 1, pp. 131-137, Jan 1981.
- [6] MacLeod, M.D., " Fast Calibration of IQ Digitizer Systems ", *Electronic Engineering*, pp. 41-45, Jan 1990.
- [7] Rice, D.W. and Wu, K.H., " Quadrature Sampling with High Dynamic Range ", *IEEE Trans. AES*, Vol. 18, No. 4, pp. 736-739, Nov 1982.
- [8] Rader, C.R., " A Simple Method for Sampling In-phase and Quadrature Components ", *IEEE Trans. AES*, Vol. 20, No.6, pp. 821-824, Nov 1984.
- [9] Bortot, P. , " Complex Demodulation Using a Digital Technique ", Technical Report, Interactive Circuits and Systems Ltd, Ottawa, Canada, Dec 1986.
- [10] Inkol, R.J., Esonu, M., Al-Khalili, D., Desormeaux, L., and Szwarc, V., " An ASIC For Wideband Signal Processing in Electronic Warfare Systems ", Proc. of the 1994 IEEE International ASIC Conference & Exhibit, Sep 19-23, 1994, Rochester, N.Y.
- [11] " HP 54520 and HP 54540 Series Oscilloscopes ", Publication no. 54542-97002, 1st edition, Aug 1993.
- [12] Dunn-Rogers, J. M., " Digital Sampling Techniques for ESM Receivers ", Proc. of the 1990 Military Microwave Conf., 1990, *IEEE Trans. AES*. Vol. AES-17, No. 1, Jan 1981.

- [13] Lee, J.P.Y., " I/Q Demodulation of Radar Signals with Calibration and Filtering ", DREO report 1119, 1991, Defence Research Establishment Ottawa, Department of National Defence, Canada.
- [14] Wiley, R.G. , *Electronic Intelligence: The Interception of Radar Signals* , 1985, Artech House Inc., Dedham, MA 02026 U.S.A.
- [15] Sharpin, D.L., Tsui, J.B.Y., and Hedge, J., " The Effects of Quadrature Sampling Imbalances on a Phase Difference Analysis Technique ", Proceedings of the IEEE, National Aerospace and Electronics Conference, NAECON 1990, Vols. 1-3; pp. 962-968, New York.
- [16] Boashash, B., Jones, G., and O'Shea, P., " Instantaneous Frequency of Signals: Concepts, Estimation Techniques and Applications ", SPIE Vol. 1152, *Advanced Algorithms and Architectures for Signal Processing IV* ,1989.
- [17] Brigham, E. Oran., *The Fast Fourier Transform*, 1974, Englewood Cliffs, New Jersey, Prentice-Hall.

## 8.0 ACKNOWLEDGEMENTS

The author would like to thank Mr. J.J. Renaud for his contribution in the design and development of the custom-matched I/Q demodulators. Thanks are also due to Mr. T. Norton for the development of the data acquisition software which greatly facilitated the measurements.

SECURITY CLASSIFICATION OF FORM  
(highest classification of Title, Abstract, Keywords)

**DOCUMENT CONTROL DATA**

(Security classification of title, body of abstract and indexing annotation must be entered when the overall document is classified)

<b>1. ORIGINATOR</b> (the name and address of the organization preparing the document. Organizations for whom the document was prepared, e.g. Establishment sponsoring a contractor's report or tasking agency are entered in section 8.) <b>DEFENCE RESEARCH ESTABLISHMENT OTTAWA</b> <b>NATIONAL DEFENCE</b> <b>SHIRLEYS BAY, OTTAWA, ONTARIO K1A 0Z4 CANADA</b>		<b>2. SECURITY CLASSIFICATION</b> (overall security classification of the document including special warning terms if applicable)  <p style="text-align: center;"><b>UNCLASSIFIED</b></p>	
<b>3. TITLE</b> (the complete document title as indicated on the title page. Its classification should be indicated by the appropriate abbreviation (S,C or U) in parentheses after the title.) <b>WIDEBAND I/Q DEMODULATORS: MEASUREMENT TECHNIQUE AND MATCHING CHARACTERISTICS (U)</b>			
<b>4. AUTHORS</b> (Last name, first name, middle initial)  <b>LEE, JIM J.P.</b>			
<b>5. DATE OF PUBLICATION</b> (month and year of publication of document)  <b>NOVEMBER 1994</b>	<b>6a. NO. OF PAGES</b> (total containing information. Include Annexes, Appendices, etc.)  <p style="text-align: center;">26</p>	<b>6b. NO. OF REFS</b> (total cited in document)  <p style="text-align: center;">17</p>	
<b>7. DESCRIPTIVE NOTES</b> (the category of the document, e.g. technical report, technical note or memorandum. If appropriate, enter the type of report, e.g. interim, progress, summary, annual or final. Give the inclusive dates when a specific reporting period is covered.)  <b>DREO REPORT</b>			
<b>8. SPONSORING ACTIVITY</b> (the name of the department project office or laboratory sponsoring the research and development. Include the address.) <b>DEFENCE RESEARCH ESTABLISHMENT OTTAWA</b> <b>NATIONAL DEFENCE</b> <b>SHIRLEYS BAY, OTTAWA, ONTARIO K1A 0Z4 CANADA</b>			
<b>9a. PROJECT OR GRANT NO.</b> (if appropriate, the applicable research and development project or grant number under which the document was written. Please specify whether project or grant)  <b>011LB</b>	<b>9b. CONTRACT NO.</b> (if appropriate, the applicable number under which the document was written)		
<b>10a. ORIGINATOR'S DOCUMENT NUMBER</b> (the official document number by which the document is identified by the originating activity. This number must be unique to this document.)  <b>DREO REPORT 1242</b>	<b>10b. OTHER DOCUMENT NOS.</b> (Any other numbers which may be assigned this document either by the originator or by the sponsor)		
<b>11. DOCUMENT AVAILABILITY</b> (any limitations on further dissemination of the document, other than those imposed by security classification)			
<input checked="" type="checkbox"/> Unlimited distribution <input type="checkbox"/> Distribution limited to defence departments and defence contractors; further distribution only as approved <input type="checkbox"/> Distribution limited to defence departments and Canadian defence contractors; further distribution only as approved <input type="checkbox"/> Distribution limited to government departments and agencies; further distribution only as approved <input type="checkbox"/> Distribution limited to defence departments; further distribution only as approved <input type="checkbox"/> Other (please specify):			
<b>12. DOCUMENT ANNOUNCEMENT</b> (any limitation to the bibliographic announcement of this document. This will normally correspond to the Document Availability (11). However, where further distribution (beyond the audience specified in 11) is possible, a wider announcement audience may be selected.)			

UNCLASSIFIED

SECURITY CLASSIFICATION OF FORM

---

**UNCLASSIFIED**

SECURITY CLASSIFICATION OF FORM

13. **ABSTRACT** ( a brief and factual summary of the document. It may also appear elsewhere in the body of the document itself. It is highly desirable that the abstract of classified documents be unclassified. Each paragraph of the abstract shall begin with an indication of the security classification of the information in the paragraph (unless the document itself is unclassified) represented as (S), (C), or (U). It is not necessary to include here abstracts in both official languages unless the text is bilingual).

(U) A simple I/Q demodulator which can be used to measure the amplitude, phase and instantaneous frequency of radar signals over a large bandwidth is investigated for electronic warfare applications. Imbalance errors and DC offsets are minimized by the techniques of component matching and calibration. A DFT technique is used to characterize the imbalances and DC offsets and improved matching characteristics on practical wideband demodulators are also given.

14. **KEYWORDS, DESCRIPTORS or IDENTIFIERS** (technically meaningful terms or short phrases that characterize a document and could be helpful in cataloguing the document. They should be selected so that no security classification is required. Identifiers, such as equipment model designation, trade name, military project code name, geographic location may also be included. If possible keywords should be selected from a published thesaurus. e.g. Thesaurus of Engineering and Scientific Terms (TEST) and that thesaurus-identified. If it is not possible to select indexing terms which are Unclassified, the classification of each should be indicated as with the title.)

**I/Q DEMODULATORS, CALIBRATION  
DIGITAL PROCESSOR**

---

**UNCLASSIFIED**

SECURITY CLASSIFICATION OF FORM

#150239

NO. OF COPIES NOMBRE DE COPIES	COPY NO. COPIE N°	INFORMATION SCIENTIST'S INITIALS INITIALES DE L'AGENT D'INFORMATION SCIENTIFIQUE
1	1	DAC
AQUISITION ROUTE FOURNI PAR	DREU	
DATE	20 Feb 95	
DSIS ACCESSION NO. NUMÉRO DSIS		

DND 1156 (8-87)



**PLEASE RETURN THIS DOCUMENT  
TO THE FOLLOWING ADDRESS:**

DIRECTOR  
SCIENTIFIC INFORMATION SERVICES  
NATIONAL DEFENCE  
HEADQUARTERS  
OTTAWA, ONT. - CANADA K1A 0K2

**PRIÈRE DE RETOURNER CE DOCUMENT  
À L'ADRESSE SUIVANTE:**

DIRECTEUR  
SERVICES D'INFORMATION SCIENTIFIQUES  
QUARTIER GÉNÉRAL  
DE LA DÉFENSE NATIONALE  
OTTAWA, ONT. - CANADA K1A 0K2